Physics Letters A 380 (2016) 1493–1498

Contents lists available at ScienceDirect

Physics Letters A

www.elsevier.com/locate/pla

Tunneling of charge carriers across a gold–squaraine interface

L.V. Govor [a,*], G. Reiter [b], J. Parisi [a]

[a] Institute of Physics, Carl von Ossietzky University of Oldenburg, D-26111 Oldenburg, Germany
[b] Institute of Physics, University of Freiburg, D-79104 Freiburg, Germany

ARTICLE INFO

Article history:
Received 21 October 2015
Received in revised form 10 February 2016
Accepted 16 February 2016
Available online 23 February 2016
Communicated by R. Wu

Keywords:
Interface metal–organic
Charge injection
Charge tunneling
Single organic crystal

ABSTRACT

We describe the transfer of holes across a gold–squaraine–gold structure via two distinct processes describing tunneling of holes through the injecting and extracting interfaces, respectively. Such separation in two steps was achieved through the evaluation of the contact resistances, derived from a decomposition of the measured total current–voltage characteristic into the corresponding components. Using the Simmons approximation, we determined the height Φ and the width d of the tunneling barrier existing at gold–squaraine interface. Interestingly, for a given gold–squaraine interface, the values of Φ and d differed for injection and extraction of holes across this interface. We attribute this difference to the action of permanent dipoles present at this interface.

1. Introduction

The fundamental property of organic devices is represented by the current–voltage (I–V) characteristic which is controlled by the injection of charge carriers at the metal–organic interface. In order to better understand the physics governing this injection process, systematic theoretical and experimental studies were carried out [1–3]. In general, organic semiconductors exhibit low electrical conductivity, because of a low density and a low mobility of the intrinsic charge carriers due to their weak coupling to molecules. That means that for obtaining a high performance of organic devices, the injection of the extrinsic charge carriers into organic semiconductor plays decisive role. Due to the energy difference between the work function of the metal and the HOMO (highest occupied molecular orbital) level of the organic material (for p-type semiconductor), an injection barrier at the metal–organic interface appears. The electric contact is expected to be ohmic if the Fermi level is close to the HOMO one [4]. Indeed, the interface barriers for charge carrier injection are not simply defined as difference between the work function of the metal and HOMO level of organic solids. It was found that due to interactions between metal and organic semiconductor, a strong interfacial dipole at the metal–organic interface forms, accompanied by an increase of the injection barrier [5,6]. As a consequence, the metal–organic interface exhibits a high contact resistance.

In our recent work [7], we attempted to achieve an ohmic contact with a squaraine (SQ) single crystal. To this end, we based our choice of the electrode material on the HOMO level estimated to be 5.3 eV [8,9]. Accordingly, we have chosen gold as the electrode material (work function of 5.2 eV). Such values would predict a rather low value of the contact resistance. However, our experiments showed that the contact resistances of gold–squaraine–gold structure were large (ranging from 10^5 to 10^8 Ω). In the present work, in order to obtain a better understanding of the physics governing hole transfer at the gold–squaraine interface, we studied tunneling of holes through the Schottky barrier existing at such interface. Here, the contact resistance was significantly larger than that of the SQ crystal (R_{sq}). Thus, we neglected the influence of the charge transport through the SQ crystal on the injection process. For the studied samples, the large contact resistances were determined using the value of R_{sq} evaluated from the samples where four-probe measurements were possible (low contact resistances). The applied procedure differed from the determination of R_{sq} described in our paper [7], but the values obtained for R_{sq} were similar in both cases. Based on our analysis, the total I–V characteristic could be decomposed into three components, describing injection and extraction of holes across gold–squaraine interface, and hole transfer through the SQ crystal. Using the Simmons approximation either in the range of low or high voltages, we determined the height and width of the tunneling barrier. Intriguingly, we observed different values of height and width for injecting and extracting holes across the same gold–squaraine interface. We attribute this difference to the action of permanent dipoles present at this interface.

* Corresponding author.
E-mail address: leonid.govor@uni-oldenburg.de (L.V. Govor).

http://dx.doi.org/10.1016/j.physleta.2016.02.025
0375-9601/

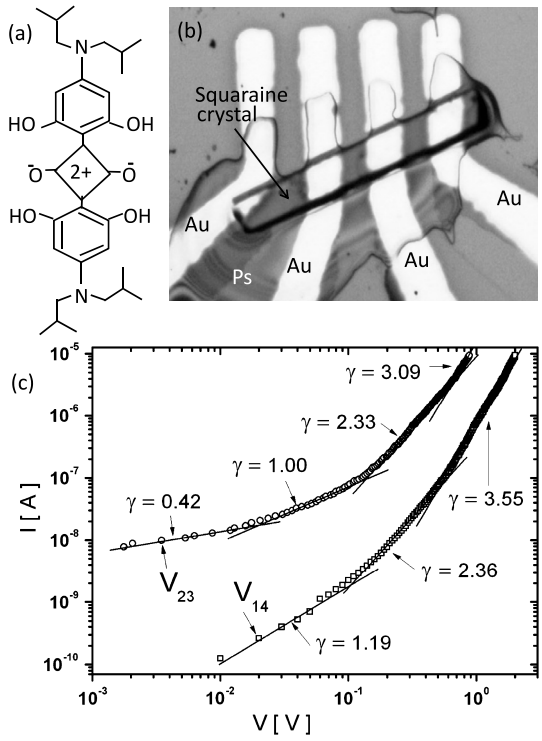

Fig. 1. (a) Chemical structure of (2,4-bis[4-(N,N-diisobutylamino)-2,6-dihydroxyphenyl]) squaraine. (b) Optical micrograph of a squaraine crystal. The size of the crystal amounts to: width $b_0 = 27$ μm, height $c_0 = 26$ μm, and length $a_0 = 240$ μm. (c) Log–log plot of the I–V characteristics measured between electrodes 1 and 4 (V_{14}), and between electrodes 2 and 3 (V_{23}), respectively. Linear fits with slope γ are shown for the ranges of the different transport regimes. All abbreviations and symbols are explained in the text.

2. Experiment

Squaraine is a dye absorbing light in the red and near-infrared spectral regions and is used as donor material in organic solar cells [10]. Figs. 1(a) and 1(b) show the chemical structure of SQ molecule and corresponding single crystal with evaporated gold electrodes (100 nm thick), respectively. The size of the SQ crystals investigated was ranged: width $b_0 = 20$–50 μm, height $c_0 = 20$–50 μm, and length $a_0 = 300$–500 μm. For each SQ crystal with four gold electrodes, a total of twelve I–V characteristics were measured at temperature of 295 K (four-, three-, and two-probe configuration for both current directions). To avoid the degradation of the crystal, we assured that the maximum current through the SQ crystal did not exceed 20 μA. At injecting electrode we applied the positive pole of the voltage. The potentials of four electrodes were denoted as V_1, V_2, V_3, and V_4, respectively. Only three of the fifteen samples investigated in total allowed reproducible measurements of the potentials V_2 and V_3 by the four-probe method (low contact resistances). We have used these samples, denoted as samples A, for the evaluation of the resistance unit of SQ crystal, R_{sq}, which was determined as resistance of crystal with the size $b_0 = 27$ μm, $c_0 = 26$ μm, and $a_0 = 24$ μm. Based on the knowledge of R_{sq}, we were able to compare the various I–V curves either measured for different electrodes on one sample or obtained for different samples.

Most samples exhibited large contact resistances. Thus, the difference V_{23} between the potentials V_2 and V_3 could not be measured with sufficient precision. For these samples, denoted as samples B, their contact resistances were determined by using the value of the specific resistivity of squaraine determined by the relation $\rho_{sq} = R_{sq} b_0 c_0 / a_0$ derived from samples A. It must be noted that after repeating measurements of the I–V curves three to five times, samples A showed approximately the behavior of samples B, i.e., they exhibited large contact resistances after repeated measurements. In contrast to samples A, the measured I–V curves of samples B were well reproducible. The behavior of samples B never changed to the one of samples A. In this work, we describe the behavior of samples B.

3. Experimental results

A representative I–V characteristic measured between electrodes 1 and 4 (V_{14}) for samples A is shown in Fig. 1(c). In addition, the corresponding dependence of the potential difference between electrodes 2 and 3 (V_{23}) on the current is presented. The data in Fig. 1(c) follow a power-law $I \sim V^{\gamma}$ with the scaling exponent $\gamma \simeq 1$, $\gamma \simeq 2.3$, and $\gamma > 3$ in the range of low, intermediate, and high voltage, respectively. Furthermore, the I–V curve with $\gamma = 0.4$ can be clearly observed for V_{23}. According to our designation, the curve V_{23} describes the SQ resistance unit R_{sq}. In this case, the measured resistance r_{14} between electrodes 1 and 4 can be written as $r_{14} = R1_{in} + R4_{ex} + 7 \times R_{sq}$. Here, the designations R_{in} and R_{ex} refer to the resistances for charge tunneling from gold to squaraine and charge tunneling from squaraine to gold, respectively. Using the value of the potential V_2, the total resistance can, thus, be separated in two partial resistances, $r_{14} = k_{12} + k_{24}$, where $k_{12} = (V_{14} - V_2)/I_{14} = R1_{in} + 2 \times R_{sq}$ and $k_{24} = V_2/I_{14} = R4_{ex} + 5 \times R_{sq}$. As a result, the injecting resistance can be calculated as $R1_{in} = k_{12} - 2 \times R_{sq}$ and extracting one as $R4_{ex} = k_{24} - 5 \times R_{sq}$. The other contact resistances can be found in a similar way. The corresponding details are described in the Supplemental Material at [11] (Determination of the contact resistances) and additionally can be found in our recent work [7].

Knowing the contact resistances, each total I–V curve measured for gold–squaraine–gold structure can be separated in three partial I–V curves describing hole injection, hole transfer along SQ crystal, and hole extraction, respectively. In general, for both current directions, the I–V curves measured between two electrodes exhibit either a symmetric or an asymmetric behavior. For example, for the two current directions, Fig. 2(a) presents the symmetric I–V characteristics measured between electrodes 3 and 4, denoted as r_{34} and r_{43}, respectively. Additionally, the corresponding partial I–V curves of the injecting contact resistance $R3_{in}$, the extracting one $R4_{ex}$, and the resistance R_{sq} are presented. Here, the x-axis refers to (a) the voltage $V3_{in}$ dropped at the resistance $R3_{in}$, (b) the voltage $V4_{ex}$ dropped at the resistance $R4_{ex}$, (c) the voltage V_{sq} dropped at R_{sq}, and (d) the voltage V_{34} applied between the electrodes 3 and 4 (curve r_{34}). For r_{43}, there are $R4_{in}$ and $R3_{ex}$, respectively. The data in Fig. 2(a) indicates that electrode 3 with contact resistances $R3_{in}$ and $R3_{ex}$ represents the dominant influence on the total I–V characteristics for r_{34} and r_{43}. Due to the equality of $R3_{in} \simeq R3_{ex}$, symmetric I–V characteristics are obtained, independent of the difference between $R4_{in}$ and $R4_{ex}$, because these values are significantly smaller. It is evident that hole transfer through the SQ crystal (R_{sq}) does not influence the total I–V characteristics measured for r_{34} and r_{43}. Similar symmetric I–V characteristics were observed between electrodes 2 and 3.

Fig. 2(b) presents an example of the asymmetric I–V characteristics measured between electrodes 1 and 2. It is evident that the asymmetry of the I–V curves for r_{12} and r_{21} is caused by electrode 1, where, firstly, the injecting $R1_{in}$ and extracting $R1_{ex}$ resistances are larger compared to those of electrode 2, and, secondly, show significantly different I–V characteristics. For r_{12}, the dominance of the resistance $R1_{in}$ is replaced by $R2_{ex}$ in the range of high voltages. As a result, a shoulder is observed on the I–V curve for r_{12}.